AIP Applied Physics Letters

Nanofluidic mixing via hybrid surface

Ziran Ye, Shunbo Li, Bingpu Zhou, Yu Sanna Hui, Rong Shen, and Weijia Wen

Citation: Applied Physics Letters **105**, 163501 (2014); doi: 10.1063/1.4898126
View online: http://dx.doi.org/10.1063/1.4898126
View Table of Contents: http://scitation.aip.org/content/aip/journal/apl/105/16?ver=pdfcov
Published by the AIP Publishing

APPLIED PHYSICS LETTERS **105**, 163501 (2014)

Nanofluidic mixing via hybrid surface

Ziran Ye,[1] Shunbo Li,[1] Bingpu Zhou,[2] Yu Sanna Hui,[2] Rong Shen,[3] and Weijia Wen[1,2]
[1]*Department of Physics, The Hong Kong University of Science and Technology, Clear Water Bay, Kowloon, Hong Kong*
[2]*Nano Science and Technology Program and Department of Physics, The Hong Kong University of Science and Technology, Clear Water Bay, Kowloon, Hong Kong*
[3]*Institute of Physics, Chinese Academy of Sciences, Beijing, China*

(Received 7 August 2014; accepted 17 August 2014; published online 20 October 2014)

We report the design and fabrication of the nanofluidic mixer comprising hybrid hydrophobic/hydrophilic micro-patterns on the top and bottom walls of the nanochannel. The unique feature of such mixer is that, without any geometric structure inside the nanochannel, the mixing can be realized solely by the hybrid surfaces. Besides, the mixing length in nanomixer has been significantly shortened comparing to micromixer. We attribute the mixing achievement to be caused by the convection and chaotic flows of two fluids along the hybrid surface due to the large surface-to-volume ratio of the nanochannel. © *2014 AIP Publishing LLC*. [http://dx.doi.org/10.1063/1.4898126]

Rapid mixing of two fluids in miniaturized devices has attracted a great deal of attention because of its potential applications in complex chemical reactions and biochemistry analysis.[1] In general, micromixing devices have channels with typical dimensions between 10 and 400 μm.[2] Without such devices, flow is considered essentially laminar at low Reynolds number (Re $<$ 100), in which the mixing process is molecular diffusion dominated and requires unacceptably long mixing lengths.[2] Microfluidic mixing usually can be divided into active mixing and passive mixing.[3–6] Active mixer relies on external perturbation energy to achieve fluidic mixing, while the passive one relies on molecular diffusion and the chaotic flow of two fluids caused by structural configuration in microchannel. A number of works have been carried out on microfluidic mixers,[7–9] and great efforts have been directed at increasing the mixing efficiency of micromixers.[10–12]

There has been no report regarding nanofluidic mixer to date due to the difficulties in nanofabrications. Active mixers require a more complex setup, passive mixers can be compact but constructing geometric structure by delicate patterning in nanochannel is very difficult. When the channel depth of a micromixer is scaled down to nanometer, in addition to the omnipresence of laminar flow conditions, as the aspect ratio (i.e., the height to width ratio) decreases, the effect of wall shear increases rapidly, leading to poor mixing.[13] On the other hand, an important feature of nanofluidics is the extremely large surface-to-volume ratio in nanochannel and the surface property becomes crucial comparing to microchannel. Therefore, the effect of channel walls becomes very significant and should be taken into account in nanofluidic mixing.

In this paper, we present an approach of nanofluidic mixer based on the fluid flowing characteristics on the top-bottom walls, which are decorated with alternating hydrophobic/hydrophilic patterns.

The nanofluidic mixer is Y-shaped, consists of nanochannel for the mixing part and microchannel for the inlet and outlet parts. Silicon and glass wafers are employed as the top and bottom walls of the nanomixer, respectively, on which the hybrid patterns with alternating hydrophobic/hydrophilic characteristics are prepared. The process flow of the chip fabrication is depicted in Figure 1. First, hexamethyldisilazane (HMDS) vapor priming was performed to make all the wafers hydrophobic. A Y-shaped channel with the width of 200 μm and a uniform depth of 640 nm was dry-etched on a smooth silicon wafer using standard photolithography technique. The designed length of the mixing part is 1 mm. After the similar HMDS pretreatment, a second photolithography process was conducted to transfer a series of hydrophilic pattern to the mixing part. Plasma treatment was performed before the removal of photoresist (PR) to make the pattern area hydrophilic. The glass wafer was processed similarly to form microchannel with the depth of 1 μm by buffered oxide etch (BOE) etching only for the inlet and outlet parts and hydrophilic pattern was coated on the mixing part. Hydrophilic pattern on the mixing part with diameter of 5 μm dot array on both silicon and glass was designed to generate vortex disturbance and induce instability to enhance mixing of the two fluids. Silicon wafer and glass wafer were then bonded using the anodic bonding technique to form a well-sealed nanofluidic device. It is noted that the hydrophilic dots on silicon and glass were staggered patterned after careful alignment under microscope (Olympus SZX16, Tokyo, Japan). The flow chart in Fig. 1 illustrates the fabrication process in detail. Fig. 2(a) shows the surface morphology of the top and bottom walls with staggered patterns in bonded nanochannel. The whole nanomixer device was completed by attaching a cured polydimethylsiloxane (PDMS, Dow Corning Corporation, Midland, USA) piece on the back side of silicon substrate along with inlet and outlet tubes.

We began the study by examining hydrophobic and hydrophilic characteristics through vapor condensation and evaporation. A silicon wafer contained designed pattern was placed on a temperature-controlled stage and monitored by a microscope (Keyence VHX-1000, Osaka, Japan). Vapor condensation was conducted by decreasing the temperature to 13 °C, followed by observation of evaporation process at this fixed temperature. As the water on the wafer evaporated, the contact line of the water receded to the pattern boundaries,

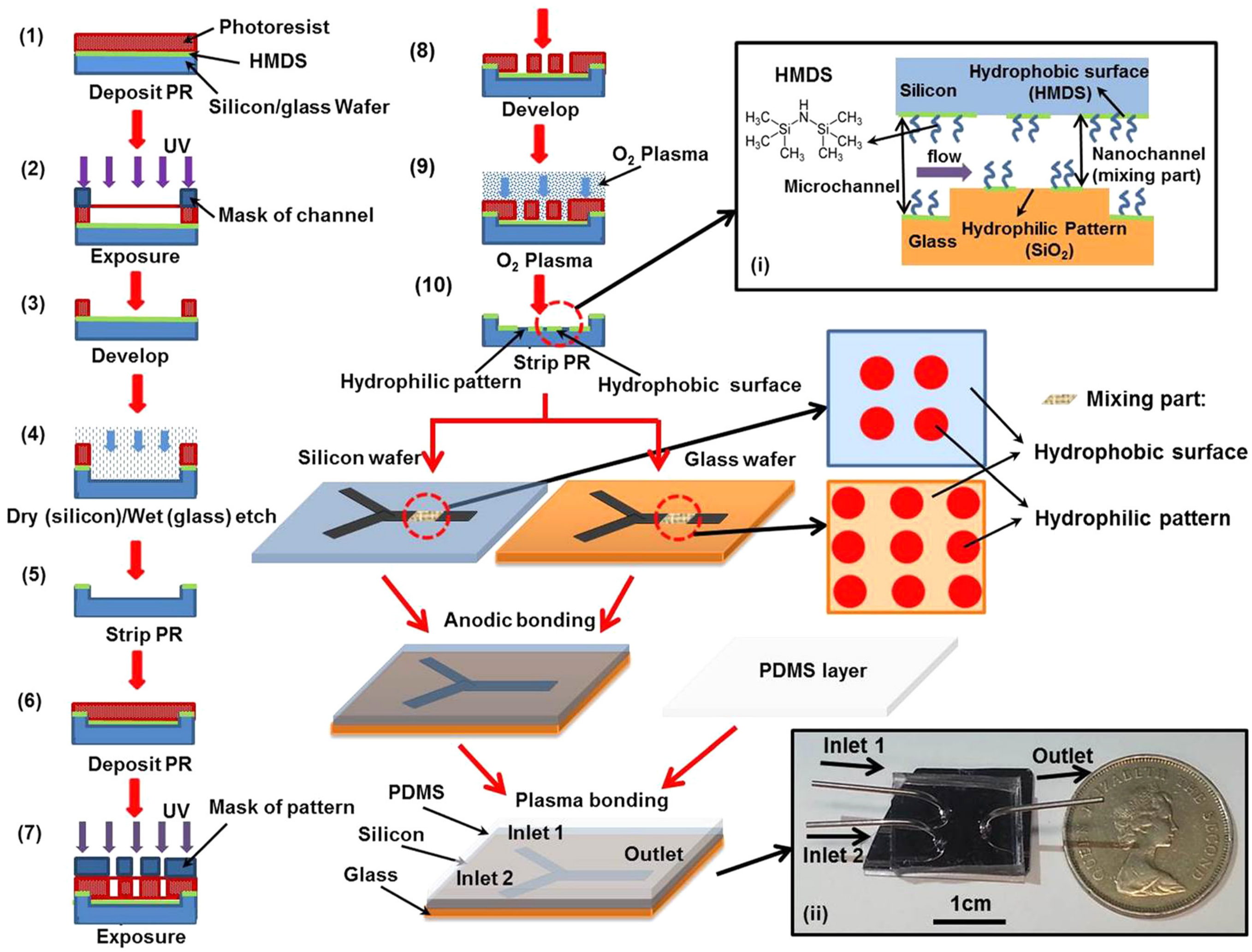

FIG. 1. Schematic illustration of the fabrication process of nanofluidic mixer including photolithography, dry/wet etching, pattern coating, aligned anodic bonding, and plasma bonding. Inset (i) and inset (ii) exhibit the longitudinal section and the optical image of the nanomixer device, respectively.

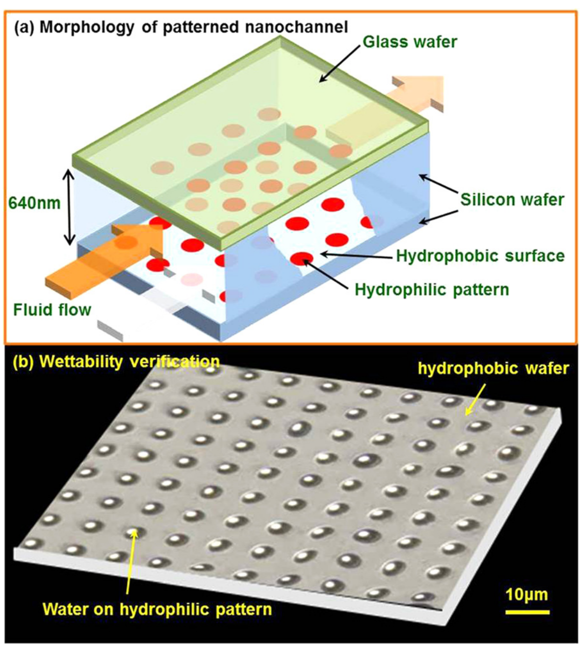

FIG. 2. (a) Morphology of patterned nanochannel. Hydrophilic patterns on the top and bottom hydrophobic walls were staggered arranged after anodic bonding process (not drawn to scale). (b) Array of water droplets on patterned silicon wafer during the evaporation process at 13 °C.

spontaneous dewetting of the hydrophobic domains and flow into the hydrophilic domains created discrete water droplets array, as shown in Fig. 2(b). These discrete droplets formed in geometries dictated by the underlying wet/nonwet surface topography, which clearly verified the hydrophobic and hydrophilic characteristics on the patterned silicon wafer.

Fluid flows of DI water and DI water dyed with Rhodamine B (10^{-2} M, Sigma-Aldrich, USA) were injected into the two branches of nanomixer through two inlets, respectively, by syringe pumps (PHD2000, Harvard Apparatus, USA), with the same pumping rate of 10 μl/h. Under our conditions, the Reynolds number was $Re < 0.1$, which indicates the domination of diffusion process at the interface. The mixing process was monitored using an inverted optical microscope (Olympus IX71, Tokyo, Japan) and recorded by a CCD camera (Olympus DP73, Tokyo, Japan).

When the two streams contacted with each other and arrived at the beginning of the patterned nanochannel, the two different-colored liquids flowed separately, remained highly and poorly fluorescent, respectively. After flowing for a distance of approximately 300 μm along the nanochannel, a notable and stable mixing was rapidly observed with an obscured flow boundary as seen in Fig. 3(a). The flows

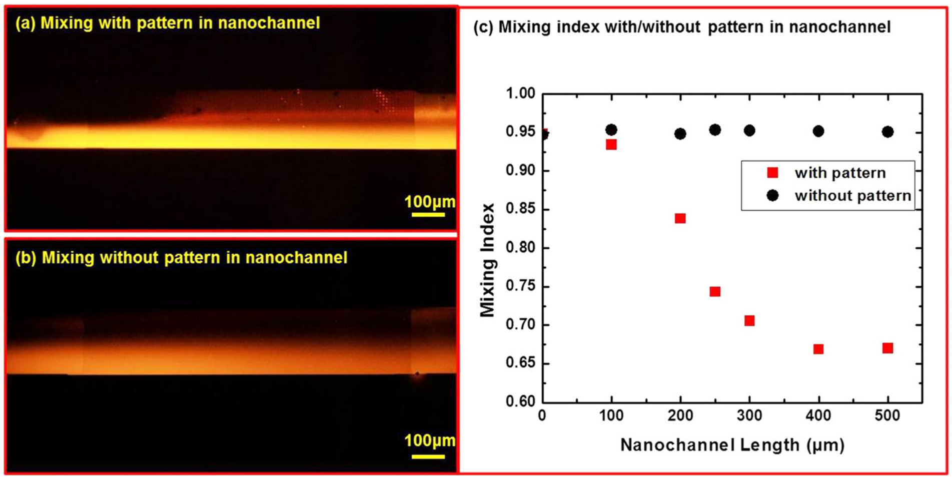

FIG. 3. (a) Mixing performance in hydrophobic nanochannel with hydrophilic pattern. (b) Mixing performance in hydrophobic nanochannel without hydrophilic pattern. (c) Comparison of mixing index in hydrophobic nanochannel with/without hydrophilic pattern.

exhibited an effective mixing by comparing the inlet and outlet flow boundaries. For comparison, mixing performance was verified in completely hydrophobic nanochannel with no hydrophilic pattern. In contrast, when the two fluids passed through the nanochannel, laminar flows were kept all along the nanochannel, as shown in Fig. 3(b).

The mixing characteristics of the images collected from experiments were analyzed using ImageJ software. From the fluorescent color intensity distribution, we evaluated the mixing index,[14] MI, using the equation $MI = \sqrt{\frac{1}{N}\sum_{i=1}^{N}\left(\frac{I_i - \langle I\rangle}{\langle I\rangle}\right)^2}$, where I_i is the intensity of pixel i, while $\langle I\rangle$ and N are the average intensity and total number of pixels, respectively. MI = 1 represents a nonmixing situation and MI = 0 defines a complete mixing of fluids. Fig. 3(c) exhibits the calculation results of MI in our experiments. At the beginning of the nanochannel, MI was almost equal to 1, indicating the complete separation of two fluids before entering the nanomixer. When the two streams of fluids passed through the nanochannel reaching a distance of $\sim$300 μm, the patterned surface on the top and bottom substrates caused a considerable decrease in MI, with the minimum value of MI = 0.67. On the contrary, after passing through the whole nanochannel in the absence of hydrophobic/hydrophilic surface decoration, MI remained almost equal to 1. These results unambiguously indicate the remarkable enhancement on mixing with hybrid surface.

Numerical simulations were also performed by Comsol Multiphysics (COMSOL 4.3a) to confirm our experimental results. The concentration distribution of two different fluids flowing through nanochannel with and without pattern is presented in Figs. 4(a) and 4(b), respectively (not drawn to scale). These figures demonstrated that a diffusion mixing layer was developed at the interface of the two fluids in both cases as the two fluids with different initial concentrations were brought into contact. The width of this mixing layer increased along the flow direction in nanochannel. However, in the case of hydrophobic nanochannel with hydrophilic patterns, the mixing process was comparatively enhanced as the flow encounters the patterned region, and the concentration variation in the yellow dashed circle area apparently indicates the mixing enhancement by pattern on the bottom wall, which validates the benefit of containing patterns on both the top and bottom walls for mixing performance.

We propose that, due to the staggered hydrophilic and hydrophobic patterns on surfaces, disturbance induced by this pattern will push the two flows to spin either clockwise or anti-clockwise and form a vortex-mixing in nanochannel. Consequently, the presence of hybrid patterns in nanochannel induces advection inside the fluid to provide a cross-stream component of velocity, which results in a better penetration of the fluids into each other to further enhance the mixing effect.

What is worth mentioning, previously reported micromixers have the typical mixing length of several to many millimeters[15] for moderate flow rates, and in a micromixer with hydrophobic/hydrophilic patterns only on the bottom wall of the microchannel,[16] effective mixing was observed after flowing for a distance of 20 mm in the microchannel. However, stable mixing phenomenon was clearly observed

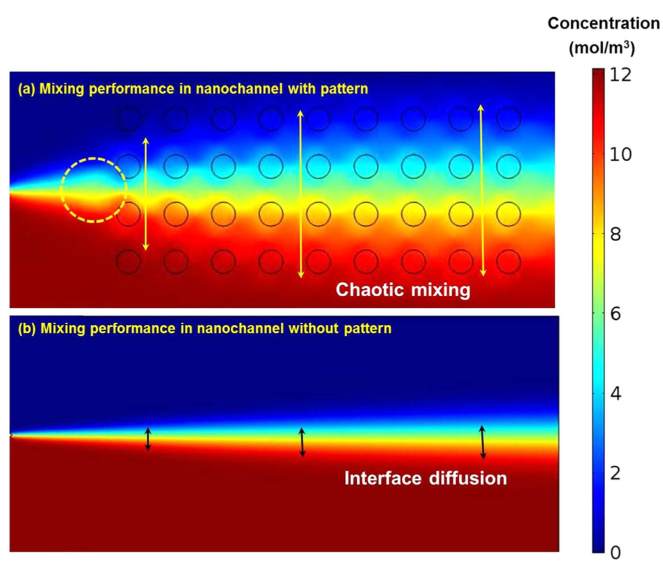

FIG. 4. (a) Simulation results of fluid concentration distribution during mixing in nanochannel with pattern (not drawn to scale). Mixing was distinguished by the variation of concentration distribution (yellow arrows). Concentration distribution affected by one of the patterns on the bottom wall was marked by a yellow dashed circle. (b) Simulation results of fluid concentration distribution during mixing in nanochannel without pattern. Development of the interface diffusion layer was marked by black arrows.

in only ~300 μm in our design, which indicates a significant reduction in mixing length. This is because, in our nanomixer, alternating hydrophilic patterns were fabricated on both the top and bottom walls of the nanochannel, which effectively increase the contact between flows and surface patterns, especially under large surface-to-volume ratio in nanochannel. For potential future work, better mixing performance is conceivable by decreasing nanochannel depth to further increase the domination of surface-related phenomena, and thus it is possible to reach a target mixing index. The limitation, however, may come from the device owing to the extremely huge pressure drop inside the nanofluidic chip.

In conclusion, using photolithography, dry/wet etching, and aligned anodic bonding techniques, we have demonstrated the nanofluidic mixer by coating hydrophilic patterns on both top and bottom walls in hydrophobic nanochannel. This nanomixer offers rapid and stable mixing performance, and has eminently shortened the mixing length comparing to micromixer. This behavior is consistent with the result of numerical analysis. Our approach provides a simple design and process for nanofluidic mixing, which should be a promising candidate for the controlled fabrication of more sophisticated nanomixer devices.

The authors wish to acknowledge the support of Hong Kong RGC grant (Grant No. HKUST604710, 605411) and National Natural Science Foundation of China (Grant No. 11290165).

[1] A. D. Stroock, S. K. W. Dertinger, A. Ajdari, I. Mezic, H. A. Stone, and G. M. Whitesides, Science **295**, 647 (2002).
[2] L. Capretto, W. Cheng, M. Hill, and X. Zhang, Top. Curr. Chem. **304**, 27 (2011).
[3] A. Venancio-Marques, F. Barbaud, and D. Baigl, J. Am. Chem. Soc. **135**, 3218 (2013).
[4] X. Z. Niu, L. Liu, W. Wen, and P. Sheng, Appl. Phys. Lett. **88**, 153508 (2006).
[5] C. C. Hong, J. W. Choi, and C. H. Ahn, Lab Chip **4**, 109 (2004).
[6] H. Chen and J.-C. Meiners, Appl. Phys. Lett. **84**, 2193 (2004).
[7] M. Long, M. A. Sprague, A. A. Grimes, B. D. Rich, and M. Khine, Appl. Phys. Lett. **94**, 133501 (2009).
[8] R. F. Ismagilov, A. D. Stroock, P. J. A. Kenis, G. Whitesides, and H. A. Stone, Appl. Phys. Lett. **76**, 2376 (2000).
[9] P. Garstecki, M. A. Fischbach, and G. M. Whitesides, Appl. Phys. Lett. **86**, 244108 (2005).
[10] K. Sritharan, C. J. Strobl, M. F. Schneider, A. Wixforth, and Z. Guttenberg, Appl. Phys. Lett. **88**, 054102 (2006).
[11] E. Y. Tafti, R. Kumar, and H. J. Cho, Appl. Phys. Lett. **93**, 143504 (2008).
[12] T. Frommelt, M. Kostur, M. Wenzel-Schäfer, P. Talkner, P. Hänggi, and A. Wixforth, Phys. Rev. Lett. **100**, 034502 (2008).
[13] P. K. Sahu, A. Golia, and A. K. Sen, Microsyst. Technol. **19**, 493 (2013).
[14] X. Mao, B. K. Juluri, M. I. Lapsley, Z. S. Stratton, and T. J. Huang, Microfluid. Nanofluid. **8**, 139 (2010).
[15] P. K. Sahu, A. Golia, and A. K. Sen, Microsyst. Technol. **18**, 823 (2012).
[16] Q. J. Cai, C. Tsai, J. DeNatale, and C. L. Chen, in *Proceeding of the 2006 ASME International Mechanical Engineering Congress and Exposition, Chicago, Illinois, USA, 5–10 November 2006*, IMECE2006-13739, p. 27.